

# Nuclear fusion

Article by:

**Post, Richard F.** Formerly, Lawrence Livermore Laboratory, Livermore, California.

**Boozer, Allen H.** Department of Applied Physics and Applied Mathematics, Columbia University, New York, New York.

**VanDevender, J. Pace** Formerly, Sandia National Laboratories, Albuquerque, New Mexico.

**Cohen, James S.** Formerly, Los Alamos National Laboratory, Los Alamos, New Mexico.

Last updated: 2014

DOI: <https://doi.org/10.1036/1097-8542.458800> (<https://doi.org/10.1036/1097-8542.458800>)

## Content

[Hide](#)

- [Properties of Fusion Reactions](#)
  - [Simple reactions](#)
  - [Cross sections](#)
  - [Energy division](#)
  - [Reaction rates](#)
  - [Critical temperatures](#)
  - [Magnetic Confinement Fusion](#)
- [Plasma configurations](#)
  - [Status](#)
  - [Physical considerations](#)
  - [Technical considerations](#)
- [Inertial Confinement Fusion](#)
  - [ICF implosions](#)
  - [ICF drivers](#)
- [Muon-Catalyzed Fusion](#)
  - [Fusion cycle](#)
  - [Yield](#)
  - [Energy balances](#)
- [Links to Primary Literature](#)
- [Additional Readings](#)

## Key Concepts

[Hide](#)

- Nuclear fusion occurs when atomic nuclei collide, forming a heavier nucleus than in the original atoms, and releasing energy in the process.
- During a nuclear fusion reaction, the attraction of the strong nuclear force must overcome the repulsion of the Coulomb force.
- Magnetic confinement fusion reactions require extremely high temperatures to convert a gas into a high-temperature plasma in which hydrogen nuclei collide and fuse together.
- Inertial confinement fusion reactions require igniting the center of a minimally heated and highly compressed fuel pellet.
- Muon-catalyzed fusion reactions occur at normal temperatures but require a high-energy muon to act as a catalyst.

**One of the primary nuclear reactions, the name usually designating an energy-releasing rearrangement collision which can occur in a collision between various isotopes of low atomic number. See also: [Nuclear reaction \(/content/nuclear-reaction/460000\)](#)**

Interest in the nuclear fusion reaction arises from the expectation that it may someday be used to produce useful power, from its role in energy generation in stars, and from its use in the fusion bomb. Since a primary fusion fuel, deuterium, occurs naturally and is therefore obtainable in virtually inexhaustible supply (by separation of heavy hydrogen from water, 1 atom of deuterium occurring per 6500 atoms of hydrogen), solution of the fusion power problem would permanently solve the problem of the present rapid depletion of chemically valuable fossil fuels. In power production the lack of radioactive waste products from the fusion reaction is another argument in its favor as opposed to the fission of uranium. See also: [Hydrogen bomb](#)

[\(/content/hydrogen-bomb/328700\)](#); [Stellar evolution \(/content/stellar-evolution/654000\)](#)

In a nuclear fusion reaction the close collision of two energy-rich nuclei results in a mutual rearrangement of their nucleons (protons and neutrons) to produce two or more reaction products, together with a release of energy. The energy usually appears in the form of kinetic energy of the reaction products, although when energetically allowed, part may be taken up as energy of an excited state of a product nucleus. In contrast to neutron-produced nuclear reactions, colliding nuclei, because they are positively charged, require a substantial initial relative kinetic energy to overcome their mutual electrostatic repulsion so that reaction can occur. This required relative energy increases with the nuclear charge  $Z$ , so that reactions between low- $Z$  nuclei are the easiest to produce. The best known of these are the reactions between the heavy isotopes of hydrogen, deuterium (D) and tritium (T). See also: [Deuterium \(/content/deuterium/189100\)](#); [Tritium \(/content/tritium/710900\)](#)

Fusion reactions were discovered in the 1920s when low- $Z$  elements were used as targets and bombarded by beams of energetic protons or deuterons. But the nuclear energy released in such bombardments is always microscopic compared with the energy of the impinging beam. This is because most of the energy of the beam particle is dissipated uselessly by ionization and interparticle collisions in the target; only a small fraction of the impinging particles actually produces reactions.

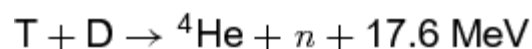
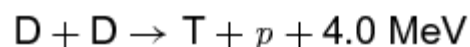
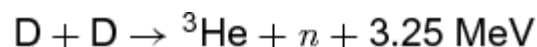
Nuclear fusion reactions can be self-sustaining, however, if they are carried out at a very high temperature. That is to say, if the fusion fuel exists in the form of a very hot ionized gas of stripped nuclei and free electrons, termed a plasma, the agitation energy of the nuclei can overcome their mutual repulsion, causing reactions to occur. This is the mechanism of energy generation in the stars and in the fusion bomb. It is also the method envisaged for the controlled generation of fusion energy. See also: [Plasma \(physics\) \(/content/plasma-physics/525900\)](#)

## Properties of Fusion Reactions

The cross sections (effective collisional areas) for many of the simple nuclear fusion reactions have been measured with high precision. It is found that the cross sections generally show broad maxima as a function of energy and have peak values in the general range of 0.01 barn (1 barn =  $10^{-28}$  m<sup>2</sup>) to a maximum value of 5 barns, for the deuterium-tritium reaction. The energy releases of these reactions can be readily calculated from the mass differences between the initial and final nuclei or determined by direct measurement.

### Simple reactions

Some of the important simple fusion reactions, their reaction products, and their energy releases are given by reactions (1) ([458800#458800RX0010](#)).



(1)

If it is remembered that the energy release in the chemical reaction in which hydrogen and oxygen combine to produce a water molecule is about 1 eV per reaction, it will be seen that, gram for gram, fusion fuel releases more than  $10^6$  times as

much energy as typical chemical fuels.

The two alternative D-D reactions listed occur with about equal probability for the same relative particle energies. The heavy reaction products, tritium and helium-3, may also react, with the release of a large amount of energy. Thus it is possible to visualize a reaction chain in which six deuterons are converted to two helium-4 nuclei, two protons, and two neutrons, with an overall energy release of 43 MeV—about  $10^5$  kWh of energy per gram of deuterium. This energy release is several times that released per gram in the fission of uranium, and several million times that released per gram by the combustion of gasoline.

## Cross sections

**Figure 1** shows the measured values of cross sections as a function of bombarding energy up to 100 keV for the total D-D reaction (both D-D,  $n$  and D-D,  $p$ ), the D-T reaction, and the D- $^3\text{He}$  reaction. The most striking characteristic of these curves is their extremely rapid falloff with energy as bombarding energies drop to a few kilovolts. This effect arises from the mutual electrostatic repulsion of the nuclei, which prevents them from approaching closely if their relative energy is small. See also: [Nuclear structure \(/content/nuclear-structure/460400\)](/content/nuclear-structure/460400)

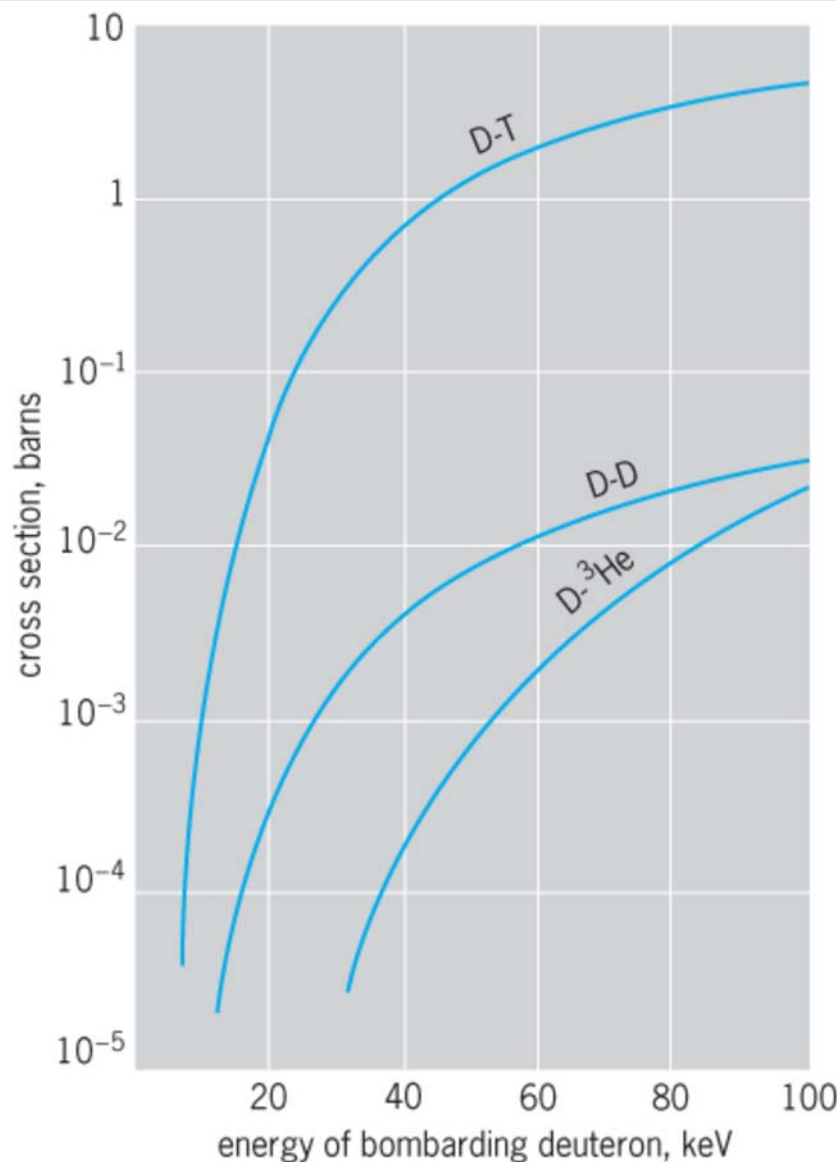


**Fig. 1** Cross sections versus bombarding energy for three simple fusion reactions. (After R. F. Post, *Fusion power, Sci. Amer.*, 197(6):73–84, December 1957)

The fact that reactions can occur at all at these energies is attributable to the finite range of nuclear interaction forces. In

effect, the boundary of the nucleus is not precisely defined by its classical diameter. The role of quantum-mechanical effects in nuclear fusion reactions has been treated by G. Gamow and others. It is predicted that the cross sections should obey an exponential law at low energies. This is well borne out in energy regions reasonably far removed from resonances (for example, below about 30 keV for the D-T reaction). Over a wide energy range at low energies, the data for the D-D reaction can be accurately fitted by a Gamow curve, the result for the cross section being given by Eq. (2),

$$\sigma_{\text{D-D}} = \frac{288}{W} \exp(-45.8/\sqrt{W}) \times 10^{-28} \text{ m}^2 \quad (2)$$

where the bombarding energy  $W$  is in kiloelectronvolts.

The extreme energy dependence of this expression can be appreciated by the fact that between 1 and 10 keV the predicted cross section varies by about 13 powers of 10, that is, from  $2 \times 10^{-46}$  to  $1.5 \times 10^{-33} \text{ m}^2$ .

## Energy division

The kinematics of the fusion reaction requires that two or more reaction products result. This is because both mass energy and momentum balance must be preserved. When there are only two reaction products (which is the case in all of the important reactions), the division of energy between the reaction products is uniquely determined, the lion's share always going to the lighter particle. The energy division (disregarding the initial bombarding energy) is as in reaction (3).



If reaction (3) holds, with the  $A$ 's representing the atomic masses of the particles and  $Q$  the total energy released, then Eqs. (4)

$$\begin{aligned} W(A'_1) + W(A'_2) &= Q \\ W(A'_1) &= Q \left( \frac{A'_2}{A'_1 + A'_2} \right) \\ W(A'_2) &= Q \left( \frac{A'_1}{A'_1 + A'_2} \right) \end{aligned} \quad (4)$$

are valid, where  $W(A'_1)$  and  $W(A'_2)$  are the kinetic energies of the reaction products.

## Reaction rates

When nuclear fusion reactions occur in a high-temperature plasma, the reaction rate per unit volume depends on the particle density  $n$  of the reacting fuel particles and on an average of their mutual reaction cross sections  $\sigma$  and relative velocity  $u$  over the particle velocity distributions. See also: [Thermonuclear reaction \(/content/thermonuclear-reaction/691500\)](#)

For dissimilar reacting nuclei (such as D and T), the reaction rate is given by Eq. (5).

$$R_{12} = n_1 n_2 \langle \sigma v \rangle_{12} \quad \text{reactions}/(\text{m}^3 \cdot \text{s}) \quad (5)$$

For similar reacting nuclei (for example, D and D), the reaction rate is given by Eq. (6).

$$R_{11} = \frac{1}{2} n^2 \langle \sigma v \rangle \quad (6)$$

Both expressions vary as the square of the total particle density (for a given fuel composition).

If the particle velocity distributions are known,  $\langle \sigma v \rangle$  can be determined as a function of energy by numerical integration, using the known reaction cross sections. It is customary to assume a Maxwellian particle velocity distribution, toward which all others tend in equilibrium. The values of  $\langle \sigma v \rangle$  for the D-D and D-T reactions are shown in **Fig. 2**. In this plot the kinetic temperature is given in kiloelectronvolts; 1 keV kinetic temperature =  $1.16 \times 10^7$  K. Just as in the case of the cross sections themselves, the most striking feature of these curves is their extremely rapid falloff with temperature at low temperatures. For example, although at 100 keV for all reactions  $\langle \sigma v \rangle$  is only weakly dependent on temperature, at 1 keV it varies as  $T^{6.3}$  and at 0.1 keV as  $T^{13.3}$ . Also, at the lowest temperatures it can be shown that only the particles in the “tail” of the distribution, which have energies that are large compared with the average, will make appreciable contributions to the reaction rate, the energy dependence of  $\sigma$  being so extreme.

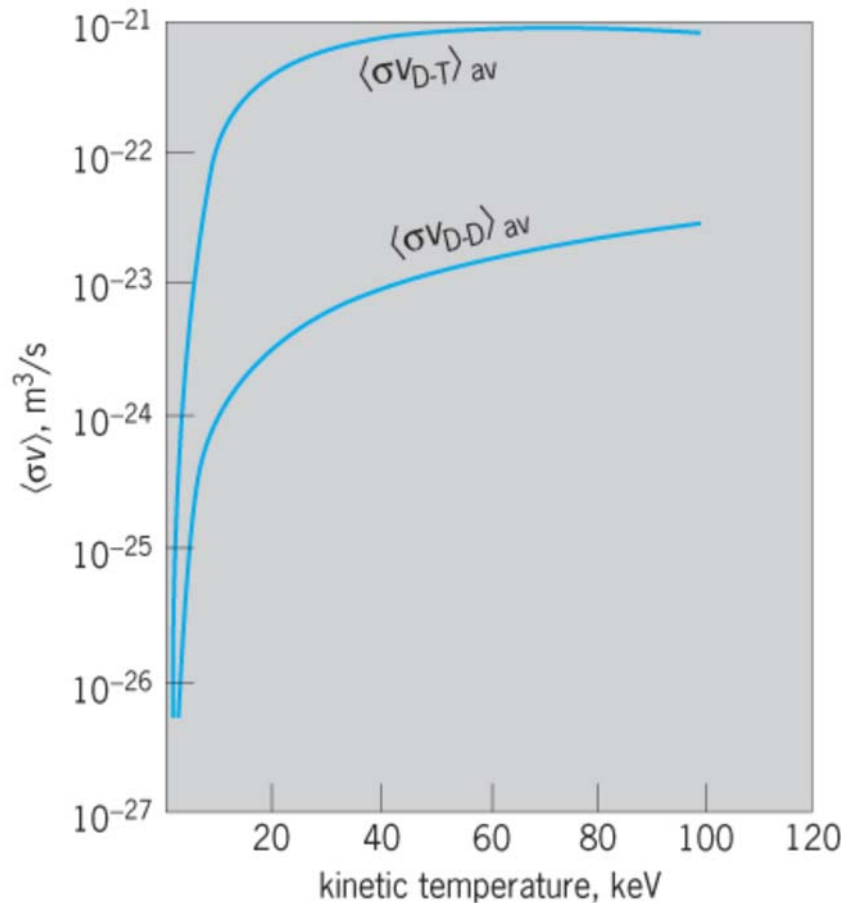


Fig. 2 Plot of the values of  $\langle \sigma v \rangle$  versus kinetic temperature for the D-D and D-T reactions.

## Critical temperatures

The nuclear fusion reaction can obviously be self-sustaining only if the rate of loss of energy from the reacting fuel is not greater than the rate of energy generation by fusion reactions. The simplest consequence of this fact is that there will exist critical or ideal ignition temperatures below which a reaction could not sustain itself, even under idealized conditions. In a fusion reactor, ideal or minimum critical temperatures are determined by the unavoidable escape of radiation from the plasma. A minimum value for the radiation emitted from any plasma is that emitted by a pure hydrogenic plasma in the form of x-rays or bremsstrahlung. Thus plasmas composed only of isotopes of hydrogen and their one-for-one accompanying electrons might be expected to possess the lowest ideal ignition temperatures. This is indeed the case: It can be shown by comparison of the nuclear energy release rates with the radiation losses that the critical temperature for the D-T reaction is about  $4 \times 10^7$

K. For the D-D reaction it is about 10 times higher. Since both radiation rate and nuclear power vary with the square of the particle density, these critical temperatures are independent of density over the density ranges of interest. The concept of the critical temperature is a highly idealized one, however, since in any real cases additional losses must be expected to occur which will modify the situation, increasing the required temperature.

Richard F. Post

## Magnetic Confinement Fusion

The application of nuclear fusion to energy production requires that the nuclear fuel have sufficient temperature, density, and confinement. If the fuel is an equal mixture of deuterium and tritium, the optimum temperature is approximately 20 keV, or  $2 \times 10^8$  °C; for other fuels the optimum temperature is even higher. At such high temperatures, atoms and molecules dissociate into ions and electrons to form a state of matter called plasma. Plasmas exhibit the same relationship between pressure  $P$ , temperature  $T$ , and the number of particles per cubic meter,  $n$ , as ordinary gases,  $P = nk_B T$ , where  $k_B$  is the Boltzmann constant. Unlike ordinary gases, such as air, plasmas are good conductors of electricity. Indeed, a fusion plasma has a conductivity more than ten times higher than copper. See also: [Boltzmann constant \(/content/boltzmann-constant/089800\)](#); [Plasma \(physics\) \(/content/plasma-physics/525900\)](#)

The high electrical conductivity of plasmas allows the fusion fuel to be confined by a magnetic field. The force per cubic meter exerted on a conductor carrying a current of density  $\mathbf{j}$  through a magnetic field  $\mathbf{B}$  is  $\mathbf{j} \times \mathbf{B}$ , which means the force is perpendicular to the current and the field. A confined plasma must have a gradient in its pressure,  $\nabla P$ , which is a force per cubic meter. Force balance, or equilibrium, between the magnetic field and plasma is achieved if Eq. (7) is satisfied.

$$\nabla P = \mathbf{j} \times \mathbf{B} \quad (7)$$

See also: [Magnetism \(/content/magnetism/398800\)](#)

Equation (7), which is the fundamental equation for magnetic confinement, constrains the shape of magnetically confined fusion plasmas to being toroidal, or doughnut-shaped. The magnetic field is perpendicular to the direction in which the pressure varies; thus, a magnetic field line can never leave a constant-pressure surface. A mathematical theorem states that only one surface shape exists in three dimensions that can everywhere be parallel to a vector, such as a magnetic field; that shape is a torus. If Eq. (7) is violated, the plasma will expand at a speed set by its sound velocity. Such plasmas are inertially confined. The efficiency of magnetic confinement is measured by the ratio of the plasma pressure  $P$  to the magnetic pressure  $B^2/2\mu_0$ , where  $\mu_0$  is the permeability of vacuum. This ratio is called beta, given by Eq. (8).

$$\beta \equiv \frac{2\mu_0 P}{B^2} \quad (8)$$

Studies of possible designs for fusion power plants have shown that a beta of approximately 5% is required for a commercially competitive plant. In these designs, a typical plasma pressure is a few times atmospheric pressure, and a typical magnetic field strength is 5 tesla, about 100,000 times greater than the magnetic field on the Earth. See also: [Magnetohydrodynamics \(/content/magnetohydrodynamics/399500\)](#)

### Plasma configurations

Although the plasma configurations used for magnetic confinement fusion are toroidal, they come in a variety of forms primarily distinguished by the strength of the net plasma current. The net plasma current flows along the magnetic field lines, and does not directly change the force balance. The net current does, however, change the magnetic field following Ampère's

law,  $\nabla \times \mathbf{B} = \mu_0 \mathbf{j}$ .

The two most prominent types of magnetic confinement devices are the tokamak and the stellarator (see [table](#)). The tokamak ([Fig. 3](#)) is toroidally symmetric and uses currents in coils to produce a strong magnetic field that encircles the torus in the toroidal direction, the long way around. A net plasma current produces a poloidal magnetic field, that is, field lines that encircle the torus the short way around. The largest tokamaks are the Joint European Torus (JET) in Britain, the JT60U in Japan, and the decommissioned Tokamak Fusion Test Reactor (TFTR) in the United States. A tokamak, ITER, which would be capable of producing fusion power at a level comparable to a power plant, has been designed under an international agreement. The design parameters are a 6.2-m (20-ft) major radius, a 2.0-m (6.6-ft) minor radius, and a 5.3-tesla magnetic field, with a planned fusion output of 500 MW. The spherical torus is a variant of the tokamak that is more compact, which means a larger ratio of the minor to the major radius of the torus.

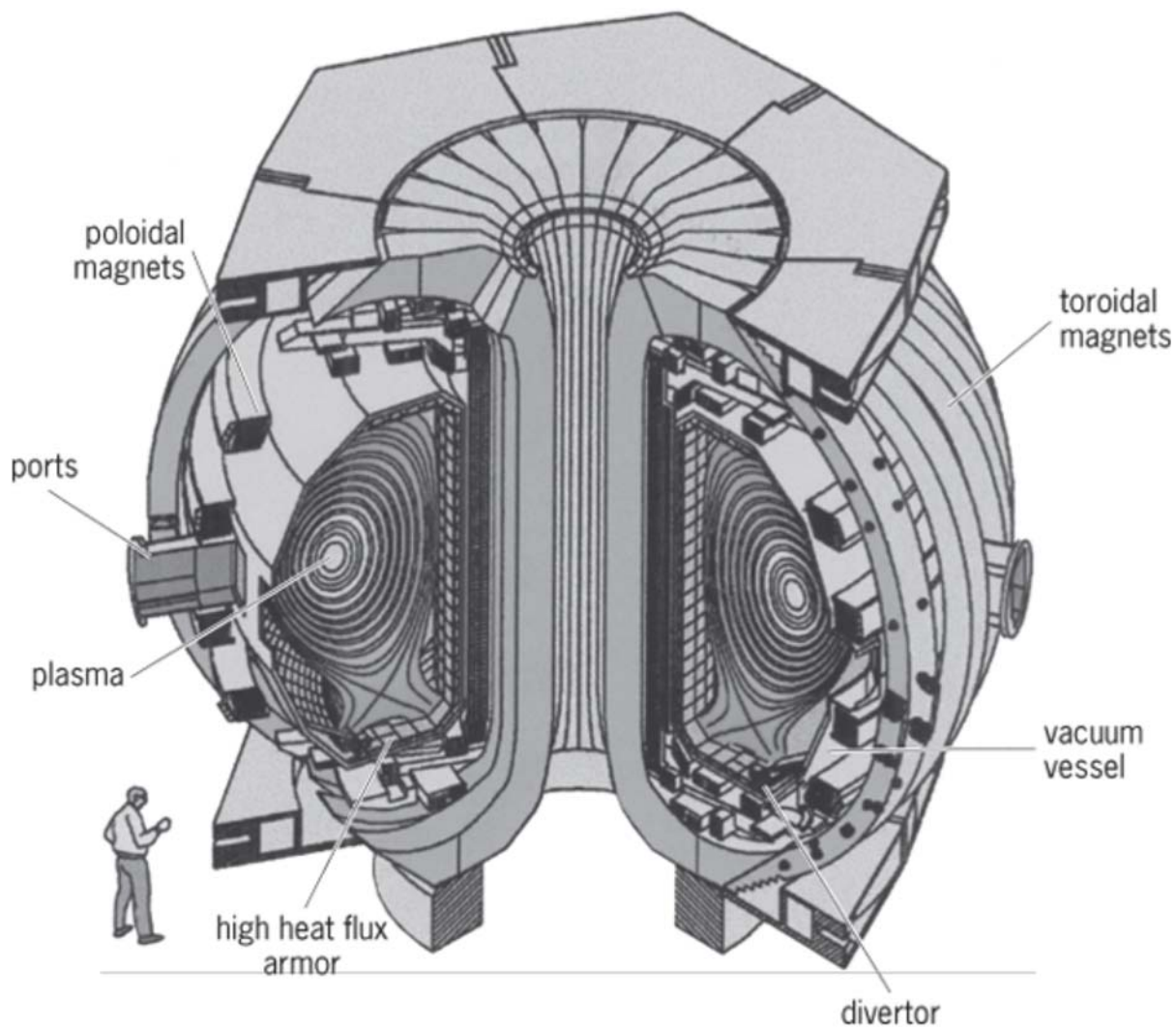


Fig. 3 Layout of the DIII-D tokamak.

Table - Some major facilities for magnetic fusion energy

Machine	Type	Location	Major radius, m(ft)	Minor radius, m(ft)	Field strength, tesla	Deuterium/tritium power, MW
DIII-D	Tokamak	United States	1.67 (5.5)	0.67 (2.2)	2.2	

Machine	Type	Location	Major radius, m(ft)	Minor radius, m(ft)	Field strength, tesla	Deuterium/tritium power, MW
JET	Tokamak	European Union	3.1 (10.2)	1.25 (4.1)	3.5	16
JT60U	Tokamak	Japan	3.4 (11.2)	1.1 (3.6)	4.2	
LHD	Stellarator	Japan	3.9 (12.8)	0.65 (2.1)	3.0	
NCSX*	Stellarator	United States	1.42 (4.7)	0.33 (1.1)	2.0	
NSTX	Spherical torus	United States	0.85 (2.8)	0.65 (2.1)	0.6	
MAST	Spherical torus	European Union	0.85 (2.8)	0.65 (2.1)	0.52	
TFTR†	Tokamak	United States	2.45 (8.0)	0.8 (2.6)	5.2	11
W7-X*	Stellarator	European Union	5.5 (18.0)	0.52 (1.7)	3.0	

\*Decommissioned.

†Under construction.

The stellarator (**Fig. 4**) requires no net plasma current to confine a toroidal plasma configuration. External coils produce field lines that lie in nested toroidal surfaces, even in the absence of a plasma. In other words, toroidal surfaces exist in the plasma region even when  $\nabla \times \mathbf{B} = 0$ . The properties of magnetic fields in a current-free region imply that the surfaces of constant pressure in a stellarator cannot be toroidally symmetric; they must have helical shaping, as must the coils that produce the field. The largest stellarator is the Large Helical Device (LHD) in Japan, which has a steady-state magnetic field produced by superconducting coils. The W7-X is a stellarator experiment of similar scale being constructed in Germany.

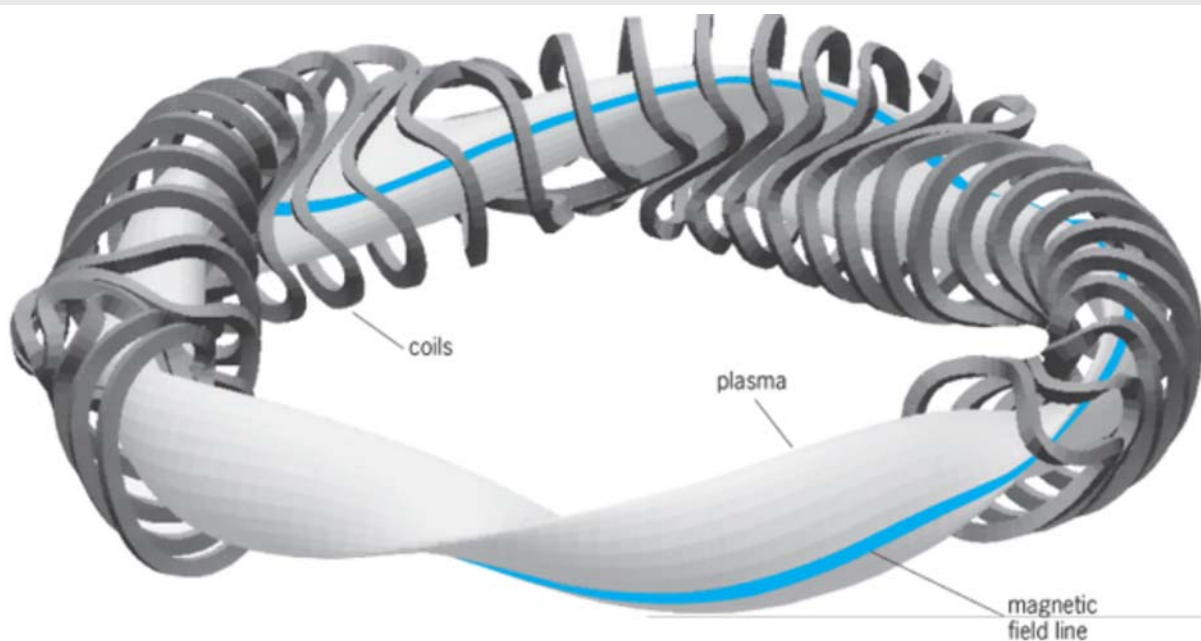


**Fig. 4** Layout of the W7-X stellarator.



## Status

Using deuterium and tritium, the JET tokamak has produced 16 MW of fusion power, which is comparable to the power required to heat the plasma (**Fig. 5**). The next generation of tokamaks should achieve the basic plasma properties required for fusion power plants. Nevertheless, the current perception of plentiful and cheap energy, especially in the United States, has led to a critical examination of the attractiveness of energy production by tokamaks and by fusion in general. The most reliable estimates indicate that electrical power produced by fusion might cost twice as much as currently available sources. In addition, a large investment in research and development is required before the technology can be shown to be practical.

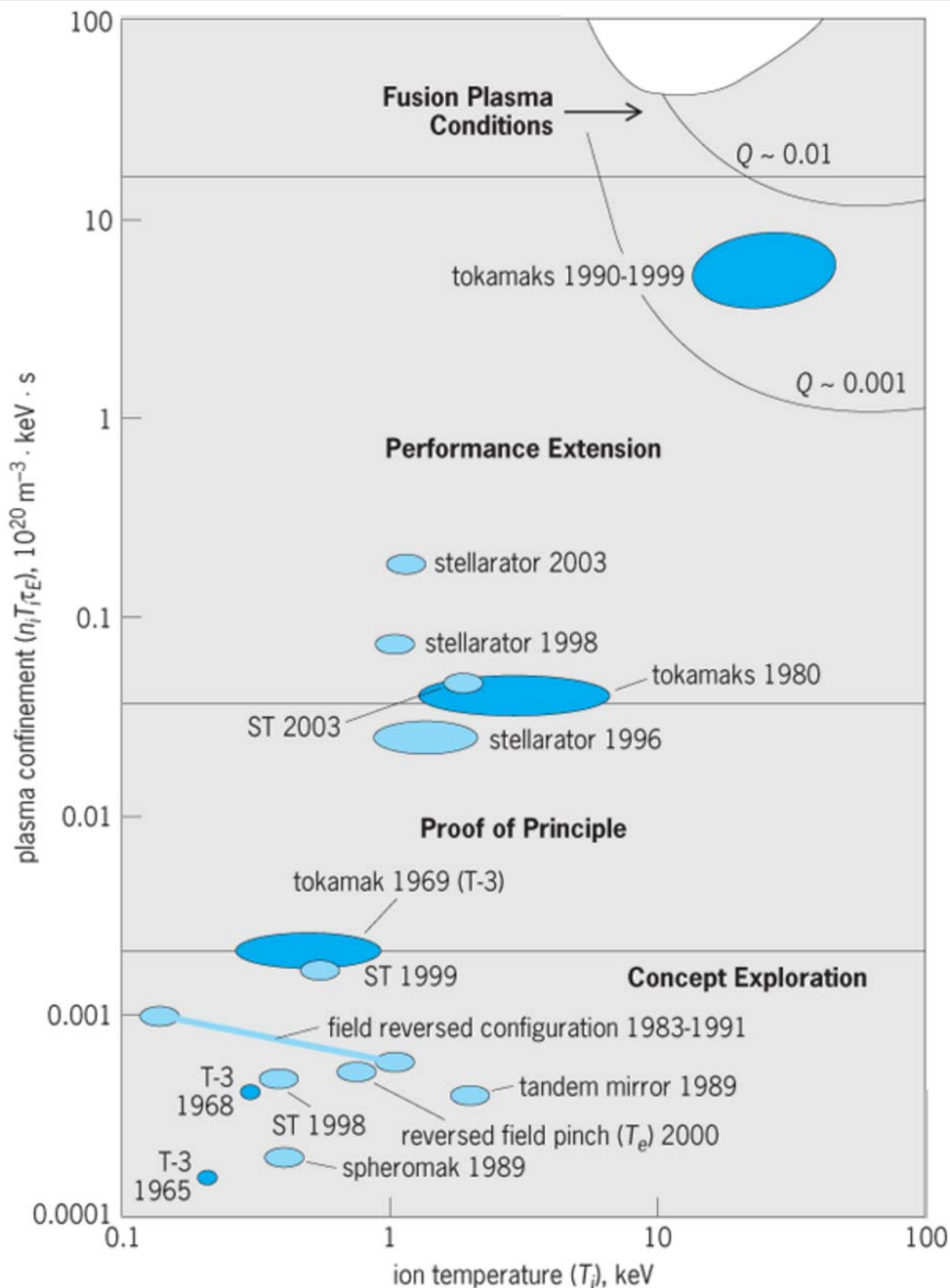


**Fig. 5 Progress in magnetic fusion.** The horizontal axis gives the plasma thermal energy, the temperature of the ions at the center of the plasma in kilovolts,  $T_i$ . One kilovolt is approximately  $12,000^\circ\text{C}$ . The vertical axis gives the plasma confinement, which is the product of the number of ions per cubic meter,  $n_i$ , the ion temperature in kilovolts,  $T_i$ , and the energy confinement time in seconds,  $\tau_E$ , which is the thermal energy in the plasma times the confinement time. The  $Q$  factors (fusion power divided by input power) are for D-D plasmas, which is the basis of most experiments. A fusion power plant would use a D-T plasma, which increases  $Q$  by an approximate factor of 400. (Dr. Dale Meade, Princeton Plasma Physics Laboratory)

The importance of fusion energy is to ensure that an unlimited source of energy can be made widely available if fossil fuels become depleted or environmentally unacceptable. The effects of depletion and environmental damage are made more

severe by the need for energy use to rise dramatically if a large fraction of the population of the world is not to remain in poverty.

## Physical considerations

Force balance [Eq. (7)] is a necessary condition for magnetic confinement, but it is not a sufficient condition. Additional issues requiring consideration are (1) the stability of the plasma equilibrium; (2) the diffusive transport of the fuel or, more importantly, its thermal energy; and (3) the loss of thermal energy through the radiation of light. For fusion using a mixture of deuterium and tritium, the third issue is primarily one of plasma purity. Heavier elements, such as carbon or iron, can radiate at a level of power far above that produced by fusion reactions. The high temperature required for fusion can be maintained only if the concentrations of impurities are carefully controlled.

### Plasma stability

The first issue, the stability of the plasma, is equivalent to asking whether the equilibrium is analogous to that of a ball at the top or the bottom of a hill. Instabilities in the force balance are of two types: those driven by the pressure gradient and those driven by the net plasma current.

Instabilities due to the pressure gradient arise from the tendency of a plasma to move to a region of lower magnetic field strength. The high conductivity of the plasma makes changing the magnetic flux embedded in an element of plasma difficult. (Magnetic flux is the strength of the magnetic field multiplied by an area transverse to the field.) By moving into a region of lower magnetic field strength, a plasma can release the free energy of expansion while conserving the embedded magnetic flux. The properties of a current-free magnetic field imply that in a torus a region of lower magnetic field strength exists in at least part of the periphery of the plasma. However, the plasma is not necessarily unstable toward moving into this region of reduced field strength (that is, the possibility of such movement is not necessarily analogous to the possibility of a ball rolling down from the top of a hill) because a magnetic field deformation is generally required in order for such movement to take place. The requirement for stability is that a deformation of the magnetic field stabilizes the plasma up to a critical value of the plasma pressure, or more precisely  $\beta$ . Values of  $\beta$  well above the minimal value for a power plant,  $\beta \approx 5\%$ , have been achieved in tokamak experiments.

The second type of instability is driven by the net current,  $j_n$ . Such instabilities are known as kink instabilities from the form of the plasma deformation that is produced. Kink instabilities limit the magnitude of the net plasma current. This limit is usually expressed using the safety factor,  $q$ , which is the number of times a magnetic field line must encircle the torus toroidally, the long way, before encircling the torus poloidally, the short way. The magnitude of the safety factor varies across the plasma. In a stable tokamak equilibrium,  $q$  is typically about 1 near the plasma center and 3 near the edge.

### Energy transport

As mentioned above, the second issue concerns the transport properties of the plasma. Although magnetically confined plasmas are in force equilibrium [Eq. (7)], they are not in thermodynamic equilibrium. Temperature gradients, which represent a deviation from thermodynamic equilibrium, lead to a transport of energy just as a temperature gradient in air does. As in air, the transport of energy in a plasma due to a temperature gradient can be much larger than that predicted by the standard transport coefficients. In air the enhancement arises from convection. In fusion plasmas the transport is due to small-scale fluctuations in the electric and magnetic fields. The enhanced transport arising from these fluctuations is called microturbulent or anomalous transport. See also: [Convection \(heat\) \(/content/convection-heat/160000\)](#); [Heat transfer \(/content/heat-transfer/311100\)](#)

The size of a fusion plasma, about 2 m (6 ft) for the smaller radius of the torus, is comparable to the size of the blankets and

shields that surround the plasma. The radial transport coefficients need to have a particular magnitude to make that radius consistent with the removal of energy from the plasma at the same rate as the plasma is heated by fusion reactions. Remarkably, the level of transport observed in experiments is close to that magnitude. Nevertheless, the uncertainties associated with microturbulent transport are among the largest uncertainties in setting the minimum size, and therefore minimum cost, for an experiment to achieve the plasma confinement required for a power plant.

Much progress has been made in the development of methods for computing microturbulent transport. Advances are paced by the development of faster computers and more sophisticated algorithms. In addition, experiments have shown that it is possible to manipulate the plasma in ways that give large reductions in microturbulent transport.

## Collisionality paradox

Fusion plasmas are in a paradoxical collisionality regime. The ions and the electrons that form a fusion plasma are said to be collisionless, since they move about 10 km (6 mi) between collisions and the plasma has a scale of only a few meters. On the other hand, fusion plasmas are highly collisional, for the energy of the ions and electrons must be confined for more than a hundred collision times. This implies that the velocity of ions and electrons obeys the same probability distribution as air molecules, the maxwellian distribution. See also: [Kinetic theory of matter \(/content/kinetic-theory-of-matter/364600\)](/content/kinetic-theory-of-matter/364600)

In a tokamak the collisionality paradox presents no fundamental problem. The toroidal symmetry of the tokamak plus the theory of hamiltonian mechanics ensure that a quantity called the toroidal canonical momentum is invariant along the trajectory of the particle. This invariance prevents the trajectories of the ions and electrons from straying far from the constant-pressure surfaces.

A stellarator cannot be toroidally symmetric, and careful design is required to ensure the confinement of particle trajectories. Surprisingly, the confinement of trajectories is controlled by the variation of the magnetic field strength in a constant-pressure surface and not by the shape of the surfaces. The surfaces of constant pressure in a stellarator cannot be toroidally symmetric, but the field strength can be almost independent of the toroidal angle in a pressure surface, and this quasi-symmetry confines the trajectories. Trajectories in a stellarator can also be confined using a subtle type of invariant of hamiltonian mechanics, the longitudinal adiabatic invariant. It is this invariant that is used to confine the particle trajectories in the W7-X stellarator. See also: [Hamilton's equations of motion \(/content/hamilton-s-equations-of-motion/307300\)](/content/hamilton-s-equations-of-motion/307300)

## Stellarator advantages

The reasons that stellarators are considered attractive for fusion are the robust stability of stellarator plasmas and the absence of a requirement for power to drive a net current. The robust stability of stellarator plasmas means they do not experience sudden terminations, which would exert a large stress on the surrounding structures. Sudden terminations, called disruptions, are observed in various operating conditions of tokamak plasmas and would not be acceptable in a power plant.

## Technical considerations

In addition to the physical constraints on the design of fusion power plants, there are technical constraints: the first wall, the blanket and shields, and the coils. The solid surface immediately surrounding the plasma is called the first wall. Suitable materials are under study. Two issues concerning the first wall have to do with the neutrons that are emitted by a fusing plasma: (1) The attractiveness of fusion depends on the first wall not becoming highly radioactive. (2) The first wall must maintain its structural integrity even though neutron bombardment tends to cause materials to swell and become brittle. A third issue is economic. Fusion power becomes cheaper the higher the energy flux that can pass through the first wall. A power flux of 5 MW/m<sup>2</sup> is a typical design value, with 80% of that power in the neutrons that are produced by deuterium/tritium fusion reactions. See also: [Radiation damage to materials \(/content/radiation-damage-to-materials\)](/content/radiation-damage-to-materials)

**/566800)**

Tritium is not naturally available. In a deuterium/tritium fusion power plant, a blanket is required to produce tritium by the bombardment of lithium with neutrons. Behind the blanket are shields to prevent neutron bombardment of the current-carrying coils. The required thickness of the blanket and shield is approximately 1.5 m (5 ft) and sets a natural size scale for a fusion power plant, which is approximately 1000 MW of electric power.

The coils that produce the magnetic field in a fusion power plant must be superconducting if the plasma  $\beta$  value is to be approximately 5%. Ordinary copper coils would dissipate far too much energy. The magnetic field produced by the coils is limited both by the properties of superconductors and by the mechanical stress,  $B^2/2\mu_0$ . A commonly used limit is that of  $\text{Nb}_3\text{Sn}$  superconductors, 12 tesla. The field in the plasma is lower, and an important efficiency factor is the ratio of the average magnetic field strength in the plasma to maximum field at a coil. A typical value for this ratio is 0.5. See also: **Superconducting devices (/content/superconducting-devices/668600)**

Allen H. Boozer

## Inertial Confinement Fusion

The basic idea of inertial confinement fusion (ICF) is to assemble highly compressed, minimally heated, 1 to 10 mg of fusion main fuel (a mixture of deuterium and tritium) around a very hot igniter plasma so that the energy released in the central igniter drives a burn wave into the surrounding main fuel to ignite it before it can expand significantly. The confinement is, therefore, accomplished by the inertia of the fuel and any surrounding tamper mass.

ICF was conceived in the nuclear weapons program shortly after lasers were invented. ICF was declassified and announced in 1972 with the first publication by John Nuckolls at Lawrence Livermore National Laboratory (LLNL) in the United States. In the subsequent four decades, the basic science of high-energy-density laboratory plasmas was developed and many approaches to ICF were proposed, researched, and evolved through international efforts in the United States, the Soviet Union, the United Kingdom, France, Japan, Germany, and China. Development of increasingly sophisticated computational simulations and experimental diagnostics permitted steady progress. In the second decade of the twenty-first century, scientists at the National Ignition Facility (NIF) at LLNL are attempting to ignite thermonuclear fuel in the laboratory for the first time. Ignition-class magnetic direct drive experiments are being readied for the Z Machine at Sandia National Laboratories in the United States. The Laser Mégajoule (LMJ) in France, a second ignition-class laser that is similar to NIF, will be driving experiments. The High Power laser Energy Research (HiPER) facility is being considered for a European inertial fusion facility to study direct drive. A newly proposed target has reinvigorated the heavy-ion fusion approach. This may be the long-awaited decade for fusion to be realized.

### ***ICF implosions***

Hydrogen bombs are ICF devices with  $10^{15}$  J yields, so the process works at a huge scale; the challenge is to produce a thermonuclear yield of  $10^8$ – $10^{10}$  J with a minimal  $10^6$ – $10^7$  J energy input. A yield of 200 MJ is equivalent to about 50 kg (100 lb) of TNT, or about 4 liters (1 gallon) of oil. This amount of energy can be contained in a facility and is potentially useful for basic and applied science, research on weapons physics and weapons effects, energy production, and production of special nuclear materials and nuclear fuels.

Assembling the laboratory ICF fuel configuration inside the ICF capsule requires a driver to provide a carefully programmed pressure source, so that a sequence of small shock waves compresses the main fuel to a 10–100 g/cm<sup>3</sup>-density shell. This shell is then accelerated to a high velocity, while the separate shocks combine into a very strong shock wave ahead of the

main fuel to strongly heat the igniter plasma. The igniter plasma is then driven to a temperature of about 4–13 keV by (1) simple compression as the main fuel implodes in hot-spot ignition, (2) a final strong shock in shock ignition, or (3) particle beams in fast ignition. Although the igniter starts self-heating at 4 keV (the minimal ignition temperature in steady state), alpha heating, which is supplementary heating from energy deposition by the helium nuclei (called alpha particles) from the DT fusion reaction, is required to get the fuel to 10–13 keV before the fuel disassembles. A strong burn wave propagates into the main fuel and high yields can be obtained before disassembly of the compressed fuel.

A laser, pulsed-power generator, or particle beam can provide the precisely programmed power source—either directly to the capsule in ablative, magnetic, or mechanical direct drive or through conversion to x-rays that subsequently drive the capsule in ablative indirect drive (**Fig. 6**). Magnetic and mechanical direct drives are less well developed and will be discussed in a later section.

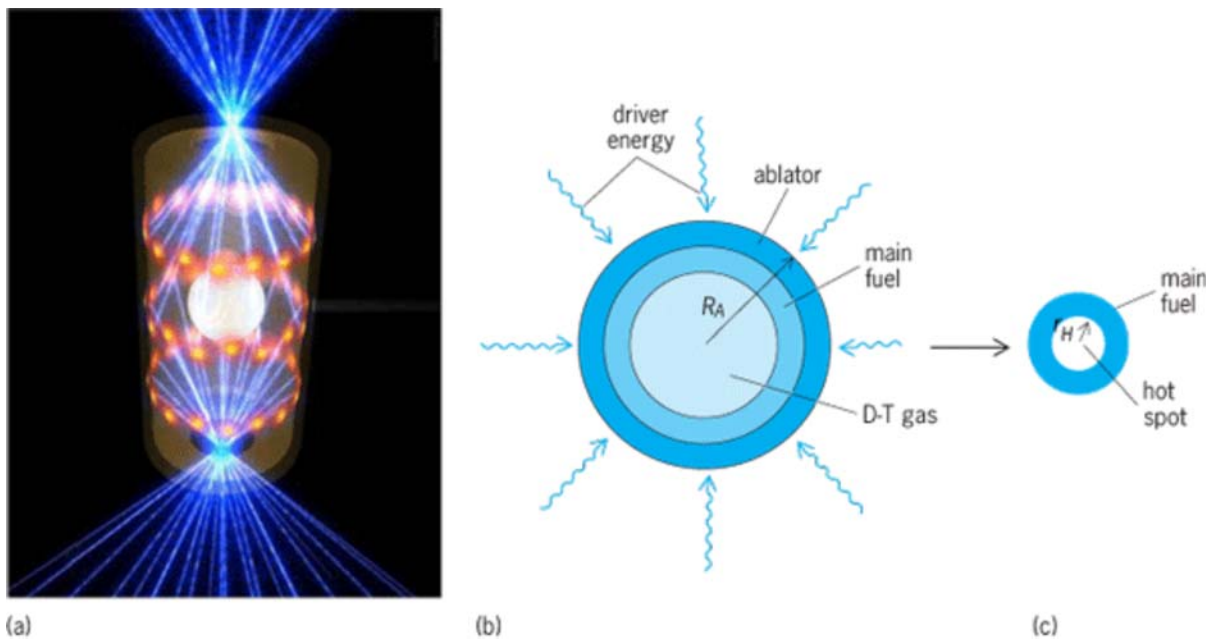


**Fig. 6** Ablative indirect drive and ablative direct drive. (a) In laser-illuminated, ablative indirect drive, the ICF target consists of a cylindrical hohlraum (hollow room) in which laser light is injected through the two holes in the end caps and heats the hohlraum wall. The resulting hot plasma produces thermal x-rays that flood the hohlraum and uniformly heat the central ICF capsule. The capsule implodes in the same manner as in ablative direct drive (Courtesy of Lawrence Livermore National Laboratory). (b) Initial and (c) final fuel configurations in ablative direct drive. Typically the convergence ratio  $R_A/r_H = 30$  to 40.

The events leading to a capsule burn with ablative drive are as follows. The laser light or x-rays deposit energy into the outer layer of the fuel-containing capsule (**Fig. 6b**). This energy deposition ablates the surface of the capsule, and the ablation acts as a rocket exhaust to generate pressures from 1 Mbar (1 million atmospheres or 100 GPa) to about 100 Mbar (10 TPa) over about 10 ns. The pressure accelerates the material of the capsule inward to velocities of approximately  $2 \times 10^5 - 4 \times 10^5$  m/s. As shown in **Fig. 7**, the inwardly directed momentum of the fuel and pusher continue to compress the fuel until it stagnates in the configuration shown in **Fig. 8** for a hot-spot-ignition capsule.

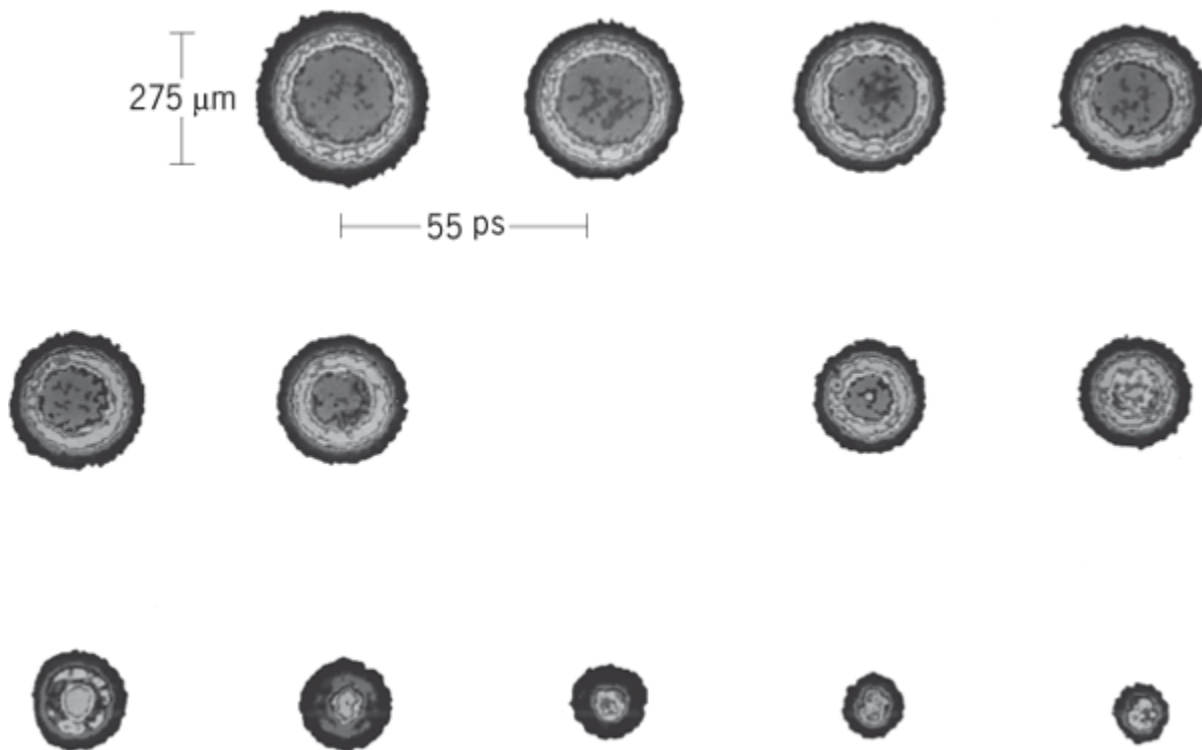


Fig. 7 X-ray images with a framing camera (developed at Lawrence Livermore National Laboratory) from a directly driven inertial confinement fusion capsule at the University of Rochester's Omega Facility. The camera has 80 ps exposure time and 55 ps time between frames. Time increases from left to right and from top to bottom.

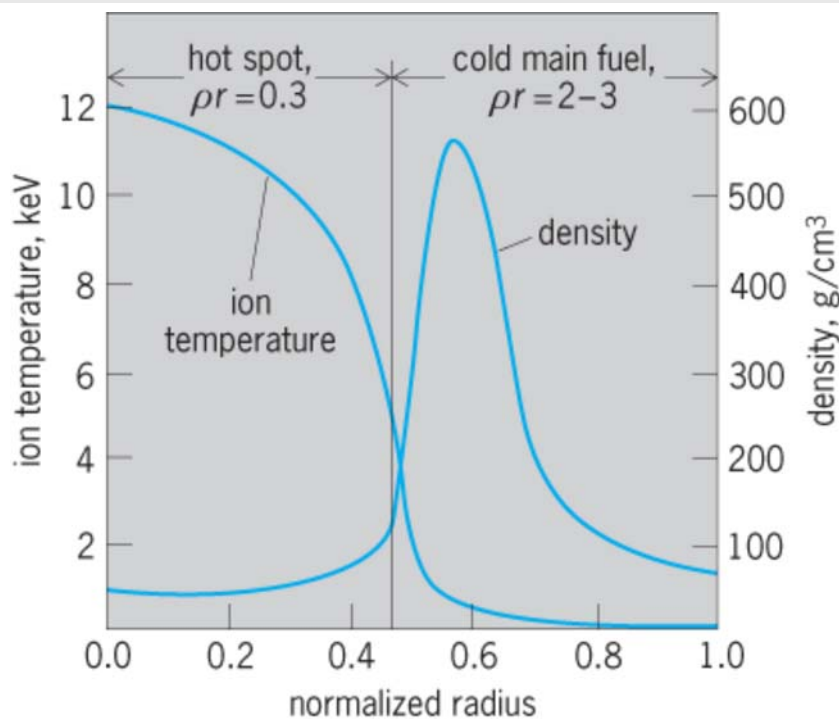


Fig. 8 Deuterium-tritium fuel ion temperature and density at ignition, plotted against normalized radius, for a typical high-gain capsule.

The product of fuel density  $\rho$  and fuel radius  $r$  is an important parameter, analogous to the  $nT_E$  product in magnetic fusion. The hot-spot value of  $\rho r$  must exceed the alpha-particle range for effective self-heating in the igniter plasma. The burn efficiency  $\eta$  for inertial confinement fusion depends on  $\rho r$  according to Eq. (9),

$$\eta = \frac{\rho r}{\rho r + 6} \quad (9)$$

where  $\rho r$  is expressed in  $\text{g/cm}^2$ . A  $\rho r$  value of  $3 \text{ g/cm}^2$  using liquid-density D-T gives 33% burn efficiency but would require about 3 kg of uncompressed D-T in a sphere. The fusion yield of that much D-T, however, is about 70 kilotons, which cannot be contained in a practical way. If the D-T fuel is compressed to 1000 times liquid density, then about 5 mg of D-T is sufficient to obtain the same  $\rho r$ , and the yield is then about 125 kg (250 lb) of TNT, which can be readily contained. Therefore, ICF necessarily requires compression to high density, which is achieved by carefully shaping the applied pressure pulse.

High compression also requires keeping x-ray and electron preheat of the fuel less than a few electron volts and requires managing hydrodynamic instabilities. Success in ICF requires nearly perfect capsules. The many advances in capsule fabrication have been an essential element in the progress of ICF. For example, capsules must be built to very tight tolerances with nearly perfect finishes (roughness of less than 50 nm) in order avoid mixing the outer portion of the shell (the ablator) with the fuel, mixing the inner portion of the shell (the pusher) with the fuel, and degrading the burn efficiency. In addition to the fabrication tolerances, pressures generated by the ablation process must be uniform to about 2% to maintain a nearly spherical implosion.

### **ICF drivers**

If the yield is at least 14 times the driver's stored energy, then inertial fusion energy with ICF might well be economically viable. Depending on which of the drivers, capsule drive modes, and ignition approaches are ultimately successful, the driver has to deliver sufficient energy, power, and intensity ( $10^6$ – $10^7$  J,  $10^{15}$  W in about 8–10 ns, and  $10^{14}$ – $10^{15}$  W/cm<sup>2</sup>) to a capsule several millimeters in diameter.

Flash-lamp pumped and laser-diode pumped neodymium:glass lasers, pulsed-power-driven current sources, electron-beam pumped krypton fluoride (KrF) lasers, and induction-linac driven heavy-ion accelerators are being developed for driving ICF capsules. Although they are at widely different stages of development, all of these technologies could probably provide a driver capable of delivering 5–10 MJ. It is not clear, however, that they can all deliver this energy while meeting the additional requirements of flexible temporal pulse shape,  $10^{15}$  W peak power, greater than  $10^{14}$  W/cm<sup>2</sup> intensity, and protecting the driver and target chamber from the explosion products.

### **National Ignition Facility (NIF)**

Flash-lamp pumped, neodymium:glass laser technology is the most developed of the four and is the driver for the 1.8-MJ NIF, which is the first facility with the mission of igniting an ICF capsule in the laboratory. Ablative indirect (x-ray driven) ICF is being explored at the NIF (**Fig. 9**).





**Fig. 9** The National Ignition Facility (NIF) at Lawrence Livermore National Laboratory (LLNL), the world's largest laser. The 1.8 MJ of ultraviolet light (351 nm wavelength from frequency-tripled neodymium:glass laser light) is generated with precision pulse shaping in the left and right laser bays and routed to the spherical target chamber in the lower center of the picture. The scale of the facility is illustrated by the fact that three American football fields could fit inside the NIF building. (Courtesy of Lawrence Livermore National Laboratory)

After the laser and core diagnostics were brought to full operational status and the hohlraum conditions were optimized by beam balancing and pointing, ignition experiments began in late 2011. Dramatic progress toward ignition by the LLNL-led team is illustrated in **Fig. 10**.

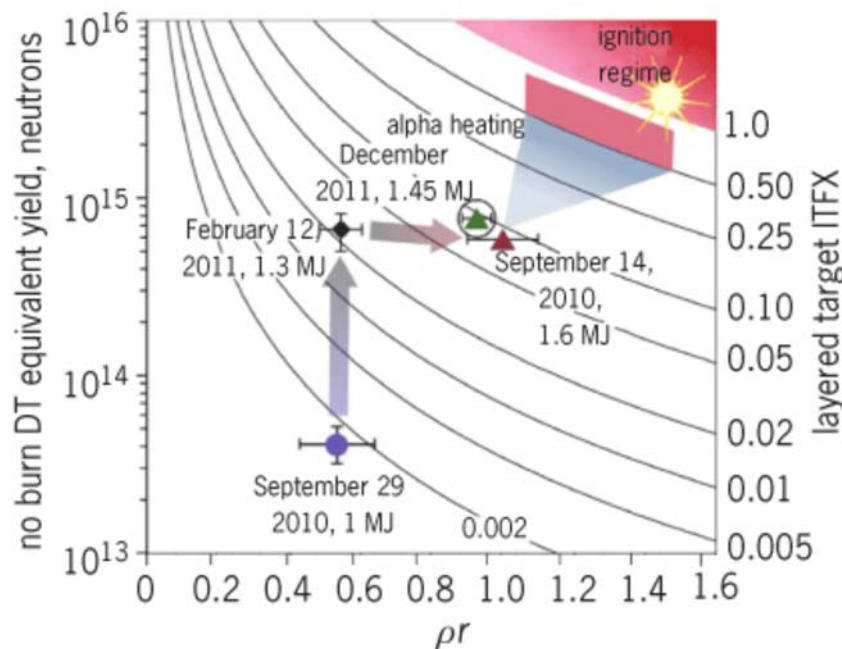


**Fig. 10** Progress toward ignition on NIF is illustrated by the plot of no-burn DT equivalent yield in number of neutrons versus the value of  $\rho r$  inferred from the energy lost by fusion neutrons during passage out of the compressed fuel. These experiments used a mixture of tritium, hydrogen, and deuterium in proportions T:H:D ~ 74:24:2, instead of equal parts of deuterium D and tritium T or D:T ~ 50:50, to enable the full suite of diagnostics to be used without being damaged by the higher yield of a DT implosion. Extracting what the yield would have been if DT were used is relatively straightforward and is shown as the no-burn DT equivalent yield on the y-axis. Results from a large number of numerical simulations of ignition-class implosions have been condensed into a single metric that can be evaluated with the measured quantities: the ignition threshold factor (ITFX), shown as contours in the plot. Values for four experiments are shown on the plot, with their dates and laser energies. (Courtesy of Lawrence Livermore National Laboratory)

In spite of the complexities and some surprises, the team has rapid progress in the first year of ignition experiments. As shown in **Fig. 10**, the integrated measure of the probability of ignition (ITFX) improved by a factor of 50 during the year. At the beginning of 2012, the team needed a factor of 6 improvement in yield and a factor of 1.5 improvement in the fuel  $\rho r$  to get into the regime of strong alpha heating and ignition.

If ignition is achieved on NIF with ablative indirect drive using the neodymium:glass laser, the NIF team has a plan for achieving high yield in the same facility. They hope to build the Laser Inertial Fusion Energy (LIFE) prototype fusion reactor with a 2-MJ, gas-cooled, diode-pumped, frequency-tripled, neodymium:glass laser to be operated at 10–15 pulses per second.

If the complexity of the problem or the inefficiency of converting laser energy to x-ray energy can be overcome by the higher efficiency of direct drive, then the NIF facility could be modified to explore polar ablative direct drive, in which uniform illumination of the capsule is obtained by optimizing the pointing and overlap of laser beams directed only from above and below the capsule. Polar direct drive is being pursued at University of Rochester's Laboratory for Laser Energetics (LLE). A much more expensive modification could allow scientists to explore uniformly illuminated direct drive.

## Z facility

The only other facility that has comparable energy and power output is Z, a 2-MJ pulsed-power-current source, which is being used to explore magnetic direct drive at Sandia National Laboratories. A cut-away illustration of Z with its companion laser Z-Beamlet and the Magnetic Liner Inertial Fusion (MagLIF) capsule are shown in **Fig. 11**.

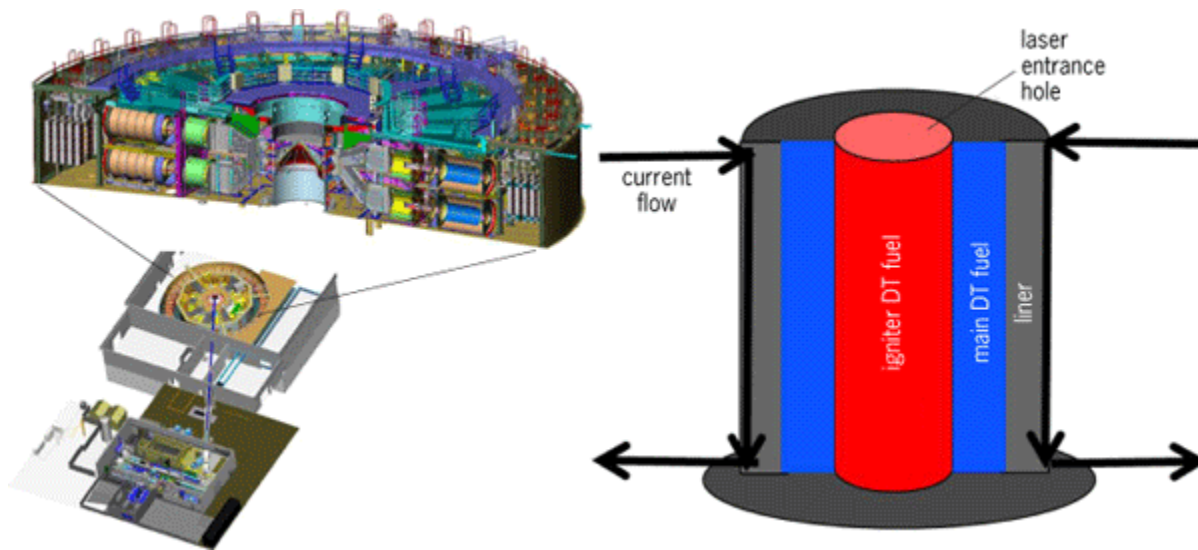


**Fig. 11** View of the combined Z Machine and Z Beamlet laser facility (lower left) with exploded view of the cross section of the Z Machine (upper left). Both will be used to drive the MagLIF capsule (right) at Sandia National Laboratories. The 10-kJ Z Beamlet laser is focused through the laser entrance hole of the MagLIF capsule to preheat the igniter plasma and the current from the 2-MJ, 27-MA Z current generator passes through the liner as shown. The associated magnetic pressure implodes the capsule. The 36-m (118-ft) diameter of the Z Machine (upper left) illustrates the scale of both Z and the Z Beamlet Laser (lower left). The diameter of the MagLIF capsule on the right is 5 mm (0.2 in.).

In computer simulations of the MagLIF capsule, a 30-tesla axial magnetic field (not shown) is generated by field coils above and below the MagLIF capsule. Then the 10-kJ laser pulse preheats the Igniter DT fuel to 250 eV as the 27 MA current from Z produces a magnetic field  $B$  outside the liner; the associated radial pressure  $P$  drives the cylindrical implosion. The pressure  $P$  for magnetic drive at a radius  $R$  in millimeters (mm) is given by Eq. (10).

$$P = \frac{B^2}{2\mu_0} = 140 \left( \frac{I_{MA}/30}{R_{mm}} \right)^2 \text{ MBar} \quad (10)$$

For comparison, the ablation pressure associated with a 300-eV hohlraum is about 140 MBar. The trapped axial magnetic field increases to 13,500 T in the simulation, reduces thermal conduction losses so that an implosion velocity of only  $1.2 \times 10^5$  m/s is sufficient, and provides some magnetic trapping of the fusion  $\alpha$  particles to reduce the required  $\rho r$  product to 0.03 to 0.08 g/cm<sup>2</sup>, depending on the density of the liner. Finally, detailed experiments on the growth of the Rayleigh-Taylor instability in magnetically driven liners on Z show that the computer simulations are highly predictive and the MagLIF design in **Fig. 11** should not be disrupted by this instability if the rms surface roughness of the liner is less than 20 nm. One-dimensional (1D) computer simulations of only the principal (radial) dynamics predict the yield (thermonuclear energy produced) is 500 kJ for Z. Similar simulations for future pulsed power drivers predict approximately 3 GJ/cm yield per unit axial length and target gain (yield divided by the sum of kinetic plus internal energy absorbed by the liner and the magnetized fuel during the implosion) of 400 for a 60-MA driver and 10 GJ/cm yield and target gain of 1000 for 70 MA.

Connecting the driver to the capsule is the major challenge for magnetic drive. A reactor must use a recyclable transmission line for coupling the current source with the fusion capsule and must replace it for every shot at a rate of once every 10 s. The cost of these recyclable lines drives the system design to large ( $\sim 10^{10}$  J) yields for economic fusion. Since curved transmission lines avoid a direct path for neutrons and debris flowing into the driver and are replaced every shot, the long-lasting walls of the reactor chamber can be protected by a flowing liquid barrier that absorbs the neutrons and debris. The recyclable transmission lines also simplify targeting because the capsule is secured to the transmission lines instead of free falling into the target zone.

## Use of KrF laser drivers

Once ignition occurs by any means, a substantial program will be needed to determine the optimum capsule and driver for single-shot, high yields (200 to 20,000 MJ) and then for repetitive yields (200 MJ at approximately 10 pulses per second to 20,000 MJ at 0.1 pulse per second) for inertial fusion energy. Ablative indirect drive with the krypton-fluoride (KrF) laser is a potential candidate for these missions and is being developed at the Naval Research Laboratory with shock ignition, which was first developed at the LLE. Krypton fluoride has advantages in that its shorter-wavelength light (248 nm) penetrates deeper into the ablator to increase the coupling efficiency and target gain (**Fig. 12**), and is less susceptible to laser-plasma instabilities.

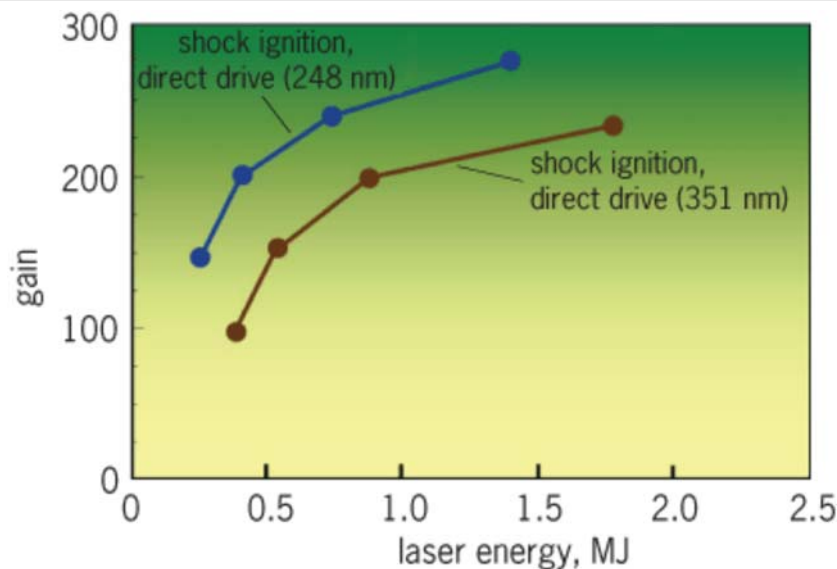


**Fig. 12** Computed capsule gains (energy yield divided by absorbed energy) from 1D simulations of the principal (radial) dynamics for ablative direct drive of a perfect capsule, which is irradiated by either 248-nm laser light or 351-nm laser light with perfect uniformity, illustrating the advantage of shorter wavelength for improved coupling efficiency. In these simulations, the focus of the laser is decreased (zoomed) during the implosion to follow the decreasing radius of the ablator. Zooming maintains the coupling efficiency and substantially reduces the laser energy for direct ablative drive.

Krypton fluoride also has a larger bandwidth than neodymium:glass, so the beams can be more easily conditioned to provide uniform illumination. Results of the Electra KrF high-repetition-rate laser (**Fig. 13**), and a system study of a future KrF reactor indicate that the cost per joule of laser energy, repetitive operability, and efficiency may also be advantageous for a KrF driver. The next step for developing a KrF driver is to design and build a full module to validate its merits for inertial fusion.

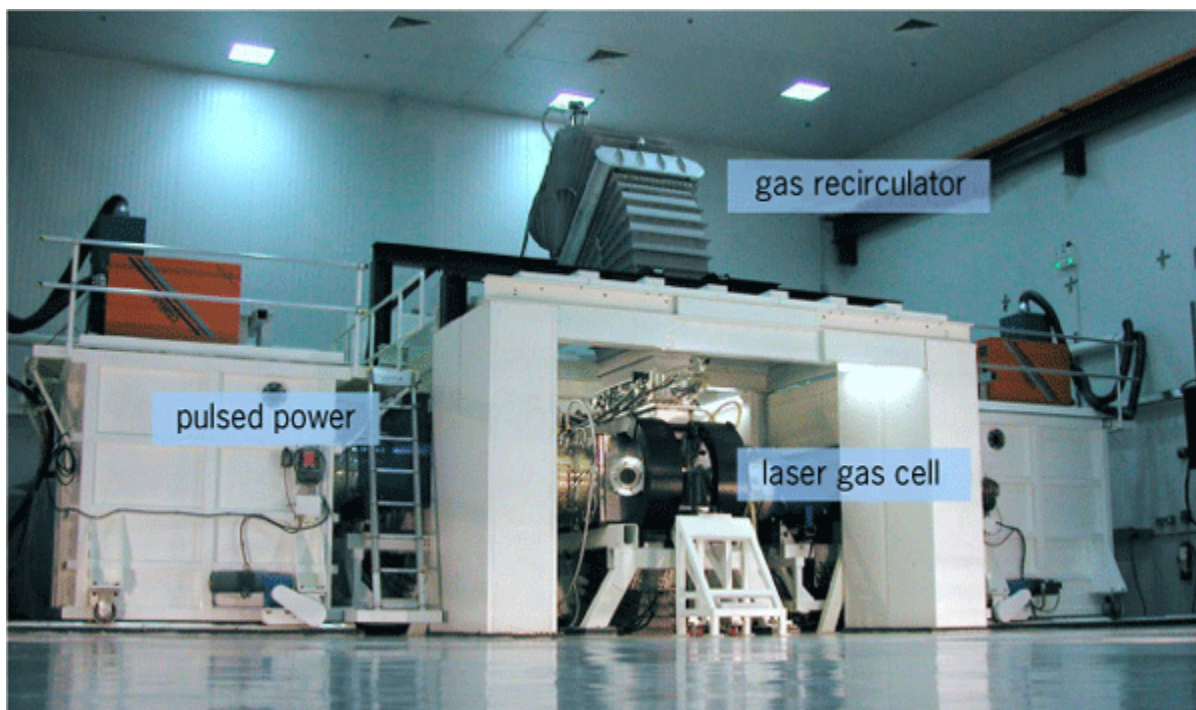


**Fig. 13** Electra, a ~500 joule/pulse, electron-beam-pumped, KrF laser at the Naval Research Laboratory. It has achieved 90,000 shots in a continuous run and 330,000 shots in eight days at 2.5–5 Hz.

## Use of heavy-ion drivers

For several decades, heavy ions were examined as a reactor driver for indirect-drive, hot-spot-ignition capsules. The relative ease of repetitive operation and standoff motivated the studies. In the first decade of the twenty-first century, the tilted X-target configuration, shown in **Fig. 14**, was invented at Lawrence Berkeley National Laboratory to fully utilize the advantages of heavy ions. The X-target is a mechanical direct-drive approach in which contained materials are heated with heavy-ion beams that have a range of  $2 \text{ g/cm}^2$ ; the resulting material pressure drives the implosion. The parameters of the three annular beams are shown in **Fig. 14**. Two annular ion beams compress the fuel and a third ion beam heats the assembled fuel for fast ignition, a concept that was invented at LLNL and demonstrated for laser driven fusion with Gekko XII at Osaka University in Japan.

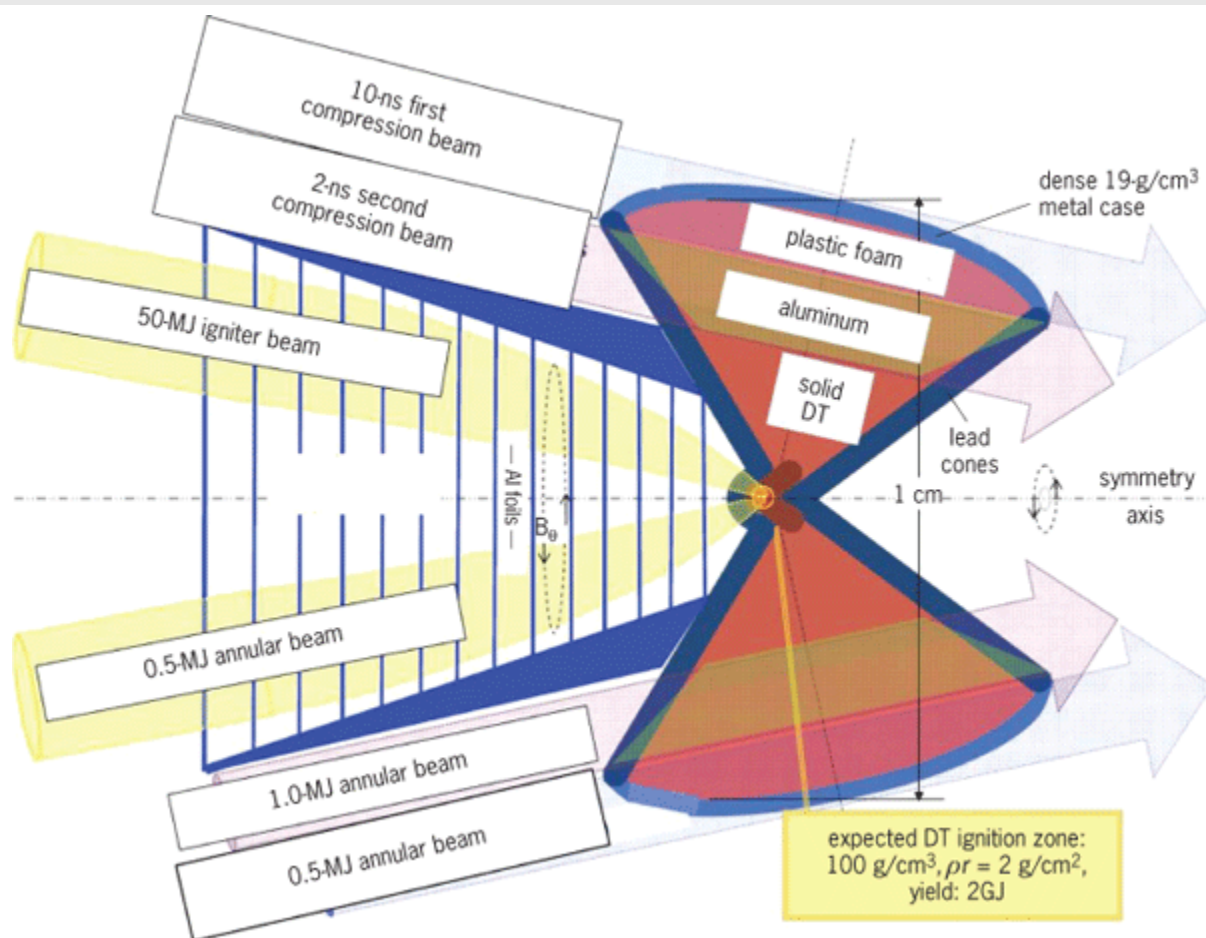


Fig. 14 Conceptual design of the X-target by the Heavy Ion Fusion Science Virtual National Laboratory.

The diversity of capsule designs, ignition mechanisms, and fusion drivers mitigates the remaining risk of failure. After forty years of work, inertial confinement fusion is on the threshold of ignition.

J. Pace VanDevender

## Muon-Catalyzed Fusion

Nuclear fusion is difficult because of the electrostatic (Coulomb) repulsion between nuclei. In traditional approaches, such as magnetic confinement and inertial confinement fusion, this barrier is overcome by energetic collisions at extraordinarily high temperatures,  $\sim 10^8$  K. In muon-catalyzed fusion, the barrier is effectively removed by binding the nuclei in an exotic molecule with a very short bond length. Fusion then occurs quickly at normal temperatures. (The process is often called cold fusion, not to be confused with the claim of cold fusion in condensed matter.) Muon-catalyzed fusion was discovered experimentally by L. A. Alvarez and collaborators in 1956 but had been hypothesized by F. C. Frank in 1947. Interest in the process as a possible energy source was rekindled by theoretical predictions in the late 1970s and experimental findings in the early 1980s.

In the normal deuterium molecule  $D_2$  or molecular ion  $D_2^+$ , with bond lengths  $\sim 10^{-10}$  m, fusion is unobservably slow (calculated to take  $\sim 10^{64}$  s). However, when the electron of  $D_2^+$  is replaced by a negative muon, the bond distance is reduced by approximately the ratio of muon to electron masses ( $m_\mu/m_e$ ), which is 207. The muon behaves like a heavy electron except that it decays with an average lifetime  $\tau_0 = 2 \times 10^{-6}$  s. The resulting small molecular ion is usually denoted  $dd\mu$  (analogously,  $D_2^+$  could be denoted  $dde$ ). Though the average distance between deuterons is still large compared with the distance where fusion can occur ( $\sim 4 \times 10^{-15}$  m), the nuclei can readily quantum-mechanically tunnel to the shorter distance. For  $dd\mu$  and  $dt\mu$  ( $d$  = deuteron =  $^2\text{H}$  and  $t$  = triton =  $^3\text{H}$ ), the times required for fusion ( $2 \times 10^{-9}$  and  $8 \times 10^{-13}$  s, respectively) are short

compared with the lifetime of the muon, though the times required to form these molecules are much longer. Muon-catalyzed fusion of nuclei with charges greater than 1 is impractical since formation of a molecule containing more than one muon is extremely improbable.

The  $d\bar{t}\mu$  molecule is of greatest interest for possible applications because fusion catalysis with it is most rapid and has least losses. A target used for high-pressure gas or liquid  $d-t$  mixtures is shown in **Fig. 15**. Muons from an accelerator are given energies such that they penetrate the steel vessel and are stopped in the fluid. The subsequent fusion neutrons also penetrate the vessel and are detected outside.

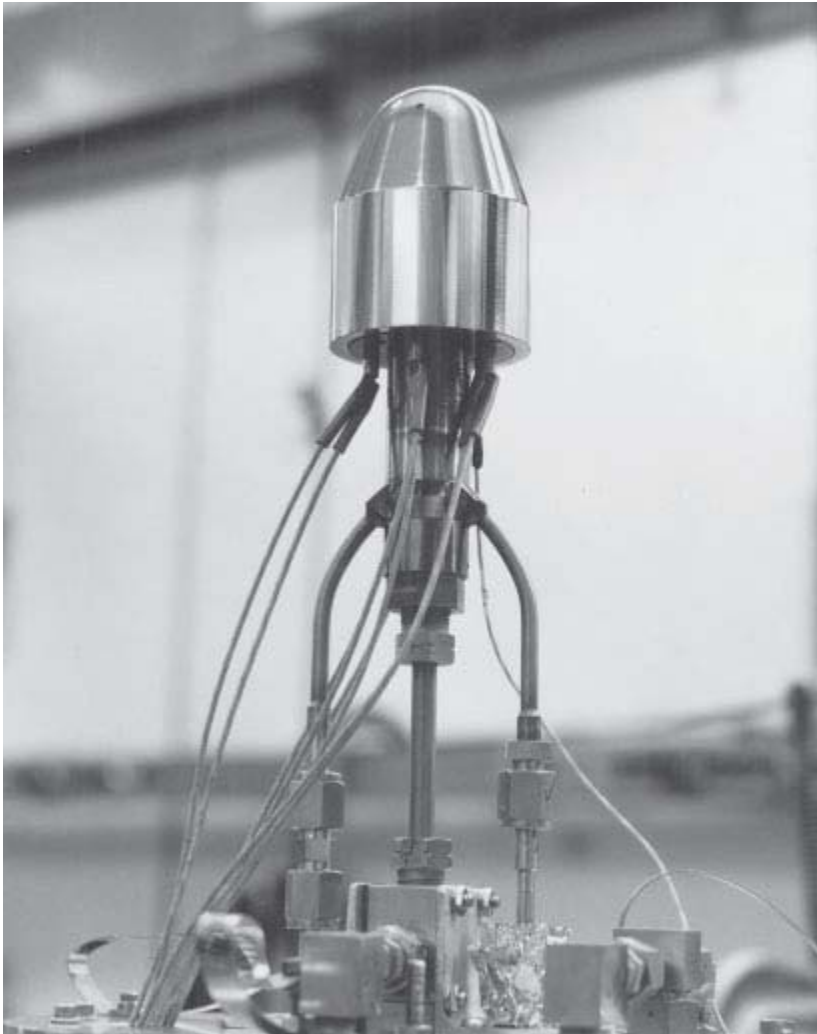


**Fig. 15** Target and connections used for muon-catalyzed fusion experiments at the Los Alamos Meson Physics Facility. The deuterium-tritium mixture is inside the high-strength stainless steel vessel [outer diameter 3 in. (7.6 cm), interior volume 2.26 in.<sup>3</sup> (37 cm<sup>3</sup>)], and the muons are incident at the rounded nose where the vessel is thinnest. The target is filled through the center stem and can be cooled by liquid helium flowing through the side tubes or heated by the four resistive heaters. The white wire goes to a temperature sensor. In the experiment, the target is surrounded by five neutron detectors. (Idaho National Engineering Laboratory)

## ***Fusion cycle***

The  $d-t$  muon-catalyzed fusion cycle (**Fig. 16**) starts with a free muon (directly from the accelerator or recycled from a previous fusion) being captured by a deuterium or tritium atom (capture occurs by displacing an electron). If initially captured by deuterium, it transfers to tritium, where it is more strongly bound. At this point an unusual mechanism allows the  $\bar{t}\mu$  atom to combine rapidly with a  $D_2$  (or D-T) molecule to form  $d\bar{t}\mu$ . A resonance is made possible by the fortuitous existence of a state of  $d\bar{t}\mu$  so weakly bound that its binding energy can go into vibrational and rotational excitation of the electronic molecule. In

this process the positively charged  $d\mu$  is so small that it acts essentially as a mass-5 hydrogenic nucleus in the electronic molecule to form a compound molecule (**Fig. 16**). After the  $d\mu$  is formed, nuclear fusion rapidly ensues, and an energetic neutron and alpha particle ( ${}^4\text{He}$ ) are emitted. Since the total time required for these events is designated  $\tau_c$ , during the lifetime  $\tau_0$  of the muon there is time for  $\tau_0/\tau_c$  cycles. See also: [Molecular structure and spectra \(/content/molecular-structure-and-spectra/431000\)](#)

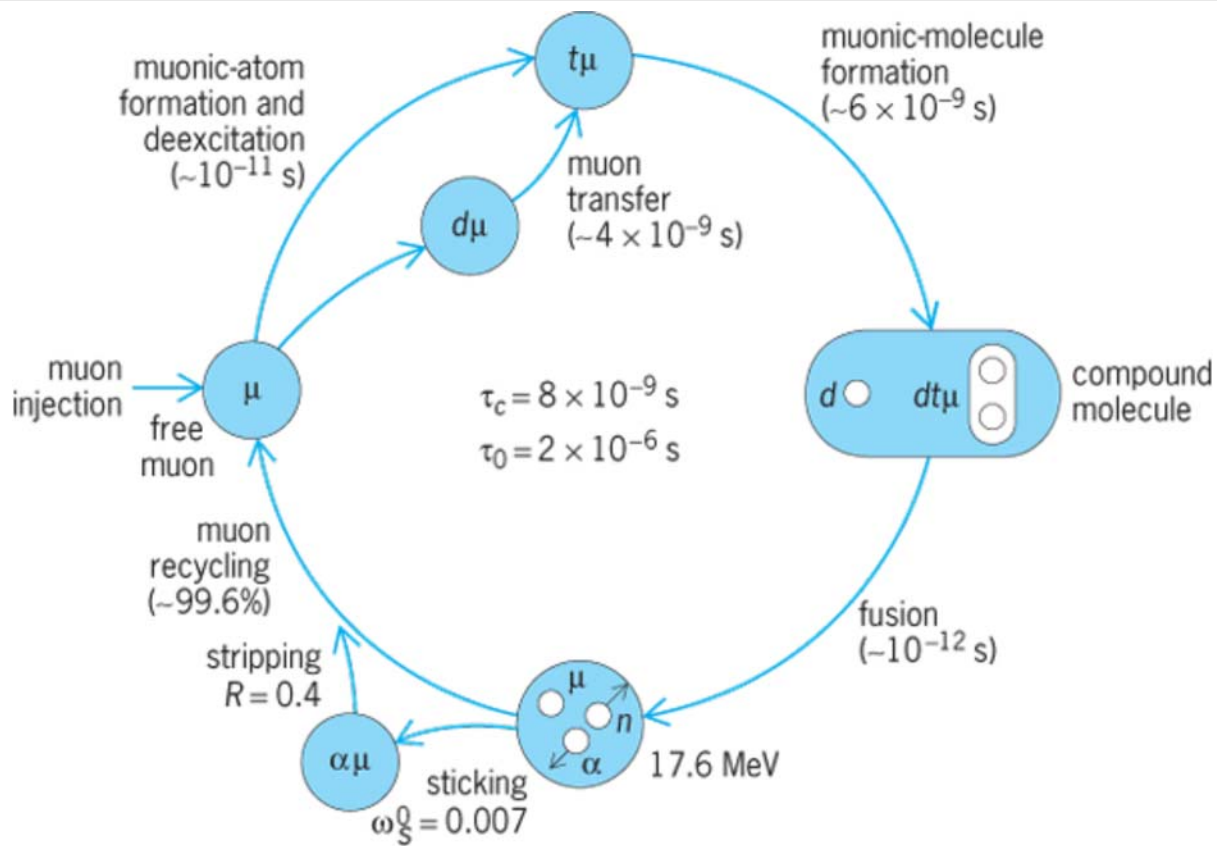


**Fig. 16** Schematic diagram of the muon-catalyzed  $d$ - $t$  fusion cycle. The approximate times indicated are for liquid-hydrogen density and tritium fraction 0.4. The muon, with lifetime  $2 \times 10^{-6}$  s, can decay at any point in the cycle.  $R$  is the fraction of initially sticking muons that are reactivated by stripping.

## Yield

Usually the muon is left behind by the fusion products to begin another catalytic cycle. However, sometimes the muon will be lost as a catalyst before it decays. This loss is primarily due to the probability  $\omega_s$  that the muon sticks to a fusion alpha particle to form a muonic helium atomic ion ( ${}^4\text{He}-\mu$ ). Hence, the average number of fusions (yield)  $Y_n$  that can be catalyzed by a single muon is given by Eq. (11).

$$Y_n = \frac{1}{\frac{\tau_c}{\tau_0} + \omega_s} \quad (11)$$

The optimum value of  $\tau_0/\tau_c$  thus far attained by experiments at temperatures up to 80°F (300 K) is  $\sim 250$  with a 60:40  $d:t$  mixture at liquid density. The measured value of  $\omega_s$  is 0.004; Eq. (11) then gives  $Y_n \approx 125$ . Further improvement would require reduction of both  $\tau_c$  and  $\omega_s$ . Experiments indicate that  $\tau_c$  is shorter at higher temperatures, and theory predicts a minimum at about 1700°F (1200 K). Application of intense electromagnetic fields to enhance stripping of the stuck muon has been proposed to reduce  $\omega_s$  (the indicated value already reflects some collisional stripping that occurs naturally).



## Energy balances

The energy generated by the number of fusions achieved thus far is not yet sufficient to recover the energy expended to make the muon. Each fusion yields 17.6 MeV of energy so that the total energy release per muon is ~2200 MeV. This is considerably greater than 106 MeV, the rest mass energy of a muon, but is still short of the ~8000 MeV required to make the muon by using present accelerator technology. Energy production would require either using less energy to make muons or more fusions per muon.

James S. Cohen

## Test Your Understanding

[Hide](#)

1. Describe the two types of hydrogen atoms used as reactants in nuclear fusion.
2. List three technical challenges in developing magnetic confinement fusion for commercial purposes.
3. Critical Thinking: How does nuclear fusion in the Sun differ from the nuclear fusion in a hydrogen bomb?

## Links to Primary Literature

A. H. Boozer, Physics of magnetically confined plasmas, *Rev. Mod. Phys.*, 76:1071–1141, 2004 DOI: <https://doi.org/10.1103/RevModPhys.76.1071> (<https://doi.org/10.1103/RevModPhys.76.1071>)

J. Rafelski and S. E. Jones, Cold nuclear fusion, *Sci. Amer.*, 257(1):84–89, July 1987 DOI: <https://doi.org/10.1038/scientificamerican0787-84> (<https://doi.org/10.1038/scientificamerican0787-84>)

S. H. Glenzer et al., Symmetric inertial confinement fusion implosions at ultra-high laser energies, *Science*, 327(5970):1228–1231, 2010 DOI: <https://doi.org/10.1126/science.1185634> (<https://doi.org/10.1126/science.1185634>)

## Additional Readings

S. Atzeni and J. Meyer-ter-vehn, *The Physics of Inertial Fusion: Beam Plasma Interaction, Hydrodynamics, and Hot Dense Matter*, International Series of Monographs on Physics 125, Oxford Science Publications, Clarendon Press, Oxford, 2004

Fusion special issue, *Euro-physics News*, vol. 29, no. 6, November/December 1998

S. E. Jones, J. Rafelski, and H. J. Mankorst (eds.), *Muon-Catalyzed Fusion*, American Institute of Physics, New York, 1989

J. D. Lindl, *Inertial Confinement Fusion: The Quest for Ignition and Energy Gain Using Indirect Drive*, Springer, New York, 1998

K. Niu, *Nuclear Fusion*, Cambridge University Press, Cambridge, U.K., 1989, reprint 2009

N. Singer, *Wonders of Nuclear Fusion: Creating an Ultimate Energy Source*, University of New Mexico Press, Albuquerque, 2011

J. Wesson et al., *Tokamaks*, 4th ed., Oxford University Press, Oxford, 2011

F. Winterberg, *The Release of Thermonuclear Energy by Inertial Confinement: Ways Towards Ignition*, World Scientific, New Jersey, 2010

C. M. Braams and P. E. Stott, *Nuclear Fusion: Half a Century of Magnetic Confinement Fusion Research*, CRC Press, Boca Raton, FL, 2010

G. McCracken and P. Stott, *Fusion*, 2d ed., Academic Press, Waltham, MA, 2013

N. Tsoulfanidis (ed.), *Nuclear Energy*, Springer Science+Business Media, New York, 2013

[Fusion Energy \(for Children\) Interactive Video \(http://ec.europa.eu/research/energy/euratom/media/video\\_fusia3d\\_en.htm\)](http://ec.europa.eu/research/energy/euratom/media/video_fusia3d_en.htm)

[Fusion Energy Educational website \(http://fused.gat.com/\)](http://fused.gat.com/)

[Fusion energy news and documents \(http://fire.pppl.gov/\)](http://fire.pppl.gov/)

[Inertial Confinement Fusion Video \(http://ec.europa.eu/research/energy/euratom/media/video\\_inertial\\_fusion\\_anim03d\\_en.htm\)](http://ec.europa.eu/research/energy/euratom/media/video_inertial_fusion_anim03d_en.htm)

[Laboratory for Laser Energetics \(http://www.lle.rochester.edu/\)](http://www.lle.rochester.edu/)

[Laser Inertial Fusion Energy \(LIFE\) \(https://life.llnl.gov/\)](https://life.llnl.gov/)

[National Ignition Campaign \(https://lasers.llnl.gov/programs/nic/\)](https://lasers.llnl.gov/programs/nic/)

[Princeton Plasma Physics Laboratory \(http://www.pppl.gov/\)](http://www.pppl.gov/)

[Proposed international tokamak ITER \(http://www.iter.org/\)](http://www.iter.org/)

[Z Machine Refurbishment \(http://www.sandia.gov/z-machine/?page\\_id=195\)](http://www.sandia.gov/z-machine/?page_id=195)